

# A new approach to landslide assessment using Depth-Number fractal model

#### ARTICLEINFO

#### Article Type Original Research

#### Author

Mohammad Ali Hadian Amri, *Ph.D.*<sup>1\*</sup> Karim Solaimani, *Ph.D.*<sup>2</sup> Ataollah Kavian, *Ph.D.*<sup>2</sup> Peyman Afzal, *Ph.D.*<sup>3</sup>

#### How to cite this article

Hadian Amri MA., Solaimani K. Kavian A., Afzal P. A new approach to landslide assessment using Depth-Number fractal model. ECOPERSIA 2023;11(1): 11-23

#### **DOR:**

20.1001.1.23222700.2023.11.1.2.2

<sup>1</sup> Assistant Professor, Department of Soil Conservation and Watershed Management, Mazandaran Agricultural and Natural Resources Research and Education Center, Agricultural Research, Education and Extension Organization (AREEO), Sari, Iran. <sup>2</sup> Professor, Department of Watershed Management Science and Engineering, Sari Agricultural Science and Natural Resources University (SANRU), Sari, Iran. <sup>3</sup> Ph.D., Department of Mining Engineering, South Tehran Branch, Islamic Azad University, Tehran, Iran.

#### \* Correspondence

Address: Mazandaran Province, Sari, 7th km of Sari to Qaemshahr road, Mazandaran Agricultural, and Natural Resources Research and Education Center. Postal Code: 4849155356, Cell Phone Number: +989119606208 Telephone Number: +981133136584 Email: m.hadian@areeo.ac.ir

### Article History

Received: July 15, 2022 Accepted: December 20, 2022 Published: February 15, 2023

#### ABSTRACT

Aims: Landslide classification using a fractal model at the Tajan river basin in northern Iran is the study intended as a new approach based on 142 landslide information data sets.

Materials & Methods: The obtained results were interpreted using the Depth–Number (Dp–N) fractal model and a relatively broad set of information available for each landslide class, consisting of the Digital Elevation Model (DEM), rainfall, land-use, geology (lithology and fault) and drainage network data.

Findings: The log-log plot shows five classes for depth (weakly, moderately, highly, strongly, and extremely magnitude) which shows that the extremely magnitude landslides have depths higher than 19.95 m in the NE, middle, western, and SE parts of the Tajan basin. The strong (5-19.95 m) and high (2.4-5 m) magnitude landslides happened in the northern, NE, western, and NW parts. The results, which were matched up to land-use, drainage network, DEM, and fault allocation patterns, revealed an affirmative correlation between landslide classes and the particulars in the area. In addition, the coefficient of determination, R2, for each population shows that the classification has been done correctly using the Dp-N fractal model. Amounts of P-value obtained from paired samples t-test and ANOVA showed that the separate categories are incongruous and significantly different (sig=0.000).

**Conclusion:** Results show that separating the populations of landslides based on a parameter as magnitude and the difference between the populations' magnitude of landslides should be considered in landslide susceptibility zonation.

Keywords: Log-log plot; Dp-N Fractal Model; Landslide Populations; Tajan River Basin.

#### CITATION LINKS

[1] Pardeshi S.D., Autade S.E., Pardeshi S.S. Landslide ... [2] Kouli M., Loupasakis C., Soupios P., Rozos D., Vallianatos F. Comparing ... [3] Zhiwang W. GIS-based methods for ... [4] Hansen A. Landslide hazard ... [5] Hansen A., Franks C.A.M. ... [6] Mandelbrot B.B. The fractal geometry of nature. W. H. Freeman, ... [7] Mandelbrot B.B. How Long Is the ... [8] Family F., Vicsek T. Dynamm ic ... [9] Turcotte D.L. Fractals and ... [10] Afzal P., Dadashzadeh Ahari H., Rashidnejad Omran N., Aliyari F. Delineation of ... [11] Turcotte D.L. A fractal ... [12] Agterberg F.P., Cheng Q., Wright D.F. Fractal ... [13] Cheng Q., Agterberg F.P., Ballantyne S.B. The ... [14] Sim B.L., Agterberg F.P., Beaudry C. Determining the ... [15] Li C., Ma T., Shi J. ... [16] Carranza E.J.M. Geochemical anomm aly and ... [17] Wang Q.F., Deng J., Wan L., Zhao J., Gong Q.J., Yang L.Q., Zhou L., Zhang Z.J. Multii fractal ... [18] Zuo R., Cheng Q., Xia Q. Application of ... [19] Afzal P., Khakzad A., Moarefvand P., Rashidnejad Omran N., Esfandiari B., Fadakar ... [20] Afzal P., Fadakar Alghalandis Y., Khakzad A., Moarefvand P., Rashidnejad ... [21] Afzal P., Fadakar Alghalandis A., Moarefvand P., Rashidd nejad ... [22] Afzal P., Alhoseini S.H., Tokhmechi B., ... [23] Malamud B.D., Turcotte D.L. The ... [24] Kubota T. A study ... [25] Omura H., Hicks L.D. Fractal dimension analysis on shallow ... [26] Omura H. Fractal dimension analysis ... [27] Tarutani N., Majtan S., Morita K., Omura H. Spatial ... [28] Majta'n S., Omura H., Morita K. Fractal ... [29] Yang Z.Y., Lee Y.H. The fractal characteristics of landslides induced by ... [30] Kubota T., Omura H., ... [31] Carranza E.J.M. Controls on mineral ... [32] Li Ch., Ma T., Sun L., Li W., Zheng A. Application and ... [33] Daneshvar Saein L., Rasa I., Rashidnejad Omran N., Moarefvand P., Afzal P. Application ... [34] Daneshvar Saein L., ... [35] Carranza E.J.M., Sadeghi M. Predictive mapping of ... [36] Cheng Q. Spatial and scaling modelling ... [37] Goncalves M.A. Characterization of ... [38] Yasrebi A.B., Wetherelt A., ... [39] Takayasu H. Fractals in the physical ... [40] Ortega O.J., Marrett R., Laubach S.E. A scale-indee pendent ... [41] Hassanpour Sh., Afzal P. Application of ... [42] Monecke T., Monecke J., Herzi P.M., ... [43] Hadian Amri M., Solaimani K., ... [44] Geology Survey ... [45] Guzzetti F., Ardizzone F., ... [46] Hadian Amri M. Landslides Susceptibility ... [47] Kelarestaghi A., Ahmadi H. Landd slide ... [48] Varnes D.J. Slope movement types and ... [49] Simonett DS Landslide distribution and ... [50] Rice R.M., Corbett E.S., ... [51] Innes J.N. Lichenometric ... [52] Guthrie R.H., Evans S.G. Analysis of ... [53] Korup O. Distribution ... [54] ten Brink U.S., Geist E.L., ... [55] Imaizumi F., Sidle R.C. Linkage of ... [56] Guzzetti F., Ardizzone F., Cardinali M., Galli M., ... [57] Imaizumi F., Sidle R.C., Kamei R. Effects of ...

#### Introduction

Landslides as a geomorphological hazard that causes significant environmental damages [1] are the second most numerous global natural catastrophic event [2]. This phenomenon is a complicated process with nonlinear inter-reaction [3]. Recognition of unstable hillside zones is one of the main aims of the landslide study. Customized geological methods for appreciation in landslide susceptibility mapping are usually based on using qualitative (direct) or quantitative (indirect) techniques [4, 5]. Recently fractal/multifractal modeling has become a proper method for studying landslides.

Fractal geometry <sup>[6]</sup> obtained by the study of self-similarity of natural features and an erratically shaped body, e.g., a coastline <sup>[7]</sup> or several other natural forms <sup>[8, 9]</sup> is the main branch of nonlinear mathematics <sup>[10]</sup>.

Fractal/multifractal modeling has been extensively used in the different branches of environmental sciences [e.g., 10,22]. Many natural hazards, e.g., earthquakes, volcanic eruptions, floods, asteroid impacts, gullies, and landslides, convince fractal frequency-size statistics to a reasonable estimate for intermediate and large events [23]. In recent years, the qualitative distribution of landslides was calculated based on fractal/multifractal modeling [24,28].

The basic fractal equation has the following form:

$$N(R) = C/RD$$
 Eq. (1)

Where N(R) is the number of items with linear dimension R, C is a constant, and D, the power of the exponential function, defines the fractal dimension.

Fractal dimension as the index of likeness, density, complexity, and frequency helps analyze susceptibility evaluation and distribution patterns and can also be used as a comparative factor. It is a good index to charac-

terize landslides' size, number, and location  $^{[29,30]}$ 

The object of this article is to propose and use the Depth-Number (Dp-N) fractal model with its relation to influential factors as the foundation for assessing landslide susceptibility.

Various geological explanations could be accessible for defining borders of different zones in landslides, which may also lead to different consequences if the physical character distribution is not considered. Euclidian geometry recognized geometrical shapes with an integer dimension, say 1D, 2D, and 3D. Though, there are a lot of other forms or spatial items, whose dimensions cannot be mathematically explained by integers but by actual numbers or fractions. These spatial objects are called fractals which describe complexity in data distribution by calculating their fractal dimensions. Different landslides can be explained based on distinctions in fractal dimensions achieved by analysis of related physical data especially the area and volume of the landslides. Fractal/multifractal modeling also demonstrates relationships between geological, hydrological, and geomorphological settings with spatial information derived from the analysis of collected data [31,34]. However, good knowledge of environmental controls is essential in categorizing hydrological and geomorphological populations based on fractal modeling [35, <sup>38, 22]</sup>. Fractals are explained by a scaling rule relating to the item being measured and the scale factor. This scaling relationship is clarified by a power law function, which explains the essential physical adjectives of the object being analyzed [39, 40]. The exponent of the power law function refers to the fractal dimensions which correspond to variations in physical adjectives such as lithology, soil type, rainfall, and structural feature [3, 32, 20, 10]. Different log-log plots in fractal models are appropriate instruments for the division of

environmental zones and classifying populations in geomorphological data, such as landslides, because threshold values can be known and assessed are shown as dividing points in those plots. These threshold values identified through fractal analysis are usually correlated with explainable field observation features or processes.

Mandelbrot (1983) proposed the Number-Size (N-S) fractal model, which is used to separation of the different geological zones and features such as islands, earthquakes, and trees. Based on the model several fractal modeling were proposed such as the concentration-number (C-N) fractal model for the separation of anomalies from the background [41]. This paper proposes the

Depth-number (Dp-N) fractal model to classify landslides.

Most studies on landslide zonation have just been based on its area without considering the depth or volume. The principal purpose of this research is to present detailed fractal geometric characteristics of 142 landslides inventory of Tajan Watershed, northern Iran by investigating the occurring conditions and inducing factors according to their spatial distribution at the basin scale and assess the fractal relationship between their depth and number as geometric characteristics to the landslides clustering and delineation; a new approach to landslide assessment and zonation worldwide which has not been used yet.

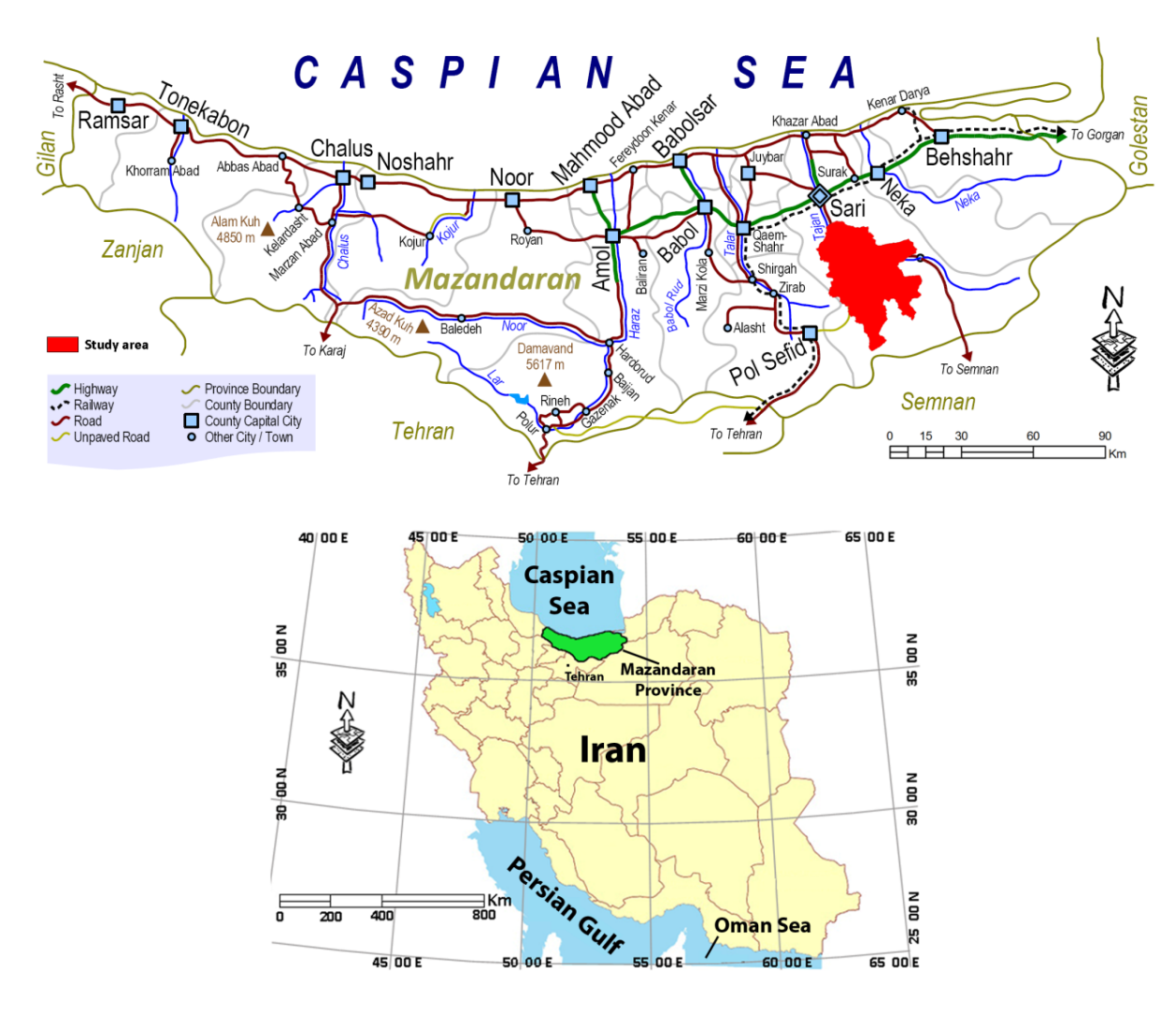


**Figure 1)** The green area on the Iran map is Mazandaran Province and the red polygon on the province map shows the area locality.

## Materials & Methods Study Area

Mazandaran Province is one of the rainiest regions in northern Iran. This province is repeatedly hit by drastic rains yearly, which generally trigger massive numeral landslides due to conditions resulting in severe casualties and economic losses. The area is in the Mazandaran province, between UTM Coordinate 680119.37E and 725053.78E, and 3986371.74N and 4041448.00N, covering approximately 1,300 km<sup>2</sup> (Figure 1). These landslides are 151 mass movements detected in the area during the local field investigations and using the Google Earth satellite images; then, according to the material and the movement types, 142 failures have been selected as landslides with rotational and translational movement types, and the material of earth. These landslides were mapped at a 1:25,000 scale. The largest and smallest landslides area is 90 ha and 180 m<sup>2</sup>, respectively (Figure 2).

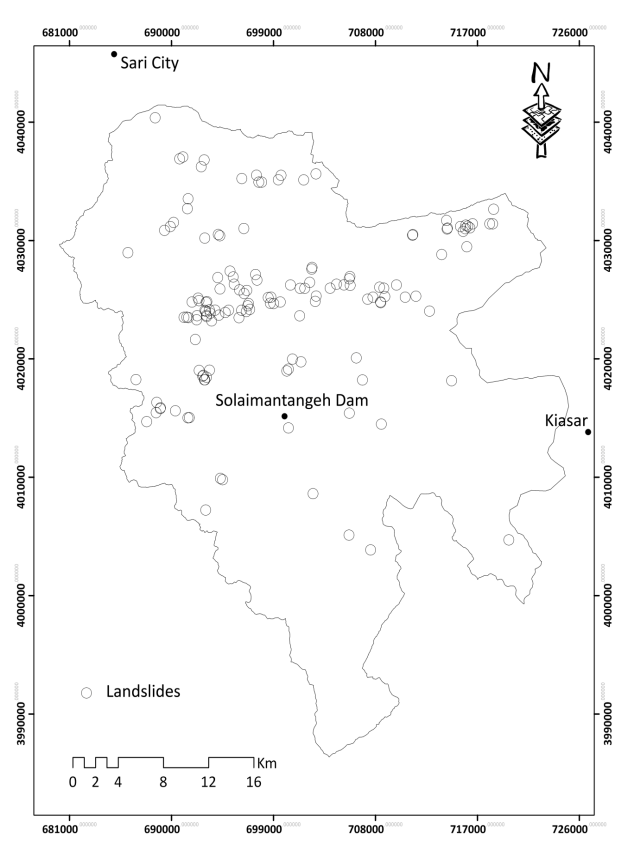


**Figure 2)** Spatial distribution of landslides in the study area.

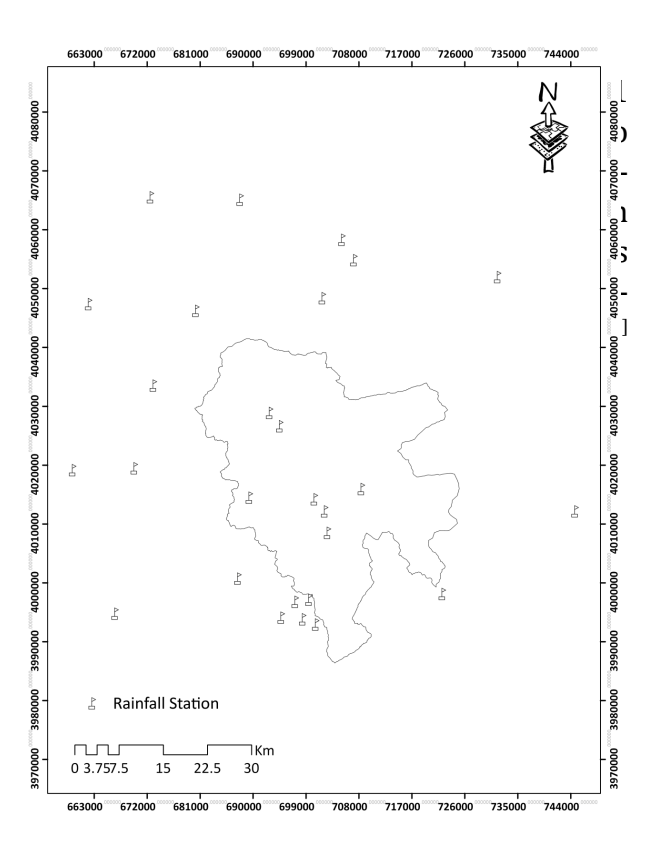


**Figure 3)** Location of the rain gauge stations used for estimating annual maximum daily rainfall (mm).

42.96% of the lithology of the area is  $M_{2,3}^{\rm m,s,l}$  group including marl, limy sandstone and siltstone, silty marl, sandy limestone, mudstone, and minor conglomerate and 15.96% of the area is covered by  $K_2^{\rm l,m}$  group including cream-light green-grey glauconitic marly limestone, limy marl, silty marl, and marl; the total length of major faults in the area is 58.17 m [44]. High and medium-density forests, mixed forest/orchards, and covers cover nearly 73% of the area.

This research was carried out to investigate the fractal model of depth-number as geometric factors of the landslide occurrence in Mazandaran province, northern Iran. The steps of the methodology used in this study are:

- 1- Extensive field surveys were accomplished to collect data on landslide points, recording the location and measuring the mean depth of existing landslide distribution.
- 2- Based on decreasing the measured values of depths, the cumulative numbers were cal-

culated for them.

3. The landslides classification have been investigated and classified by carrying out a Dp-N fractal/multifractal analysis to understand dangerous landslides based on their depth (related to area and volume), which is the primary parameter for determination of landslides' magnitude [45].

The general form of the model is

$$N(\geq \rho) \propto \rho^{-D}$$
 Eq. (2)

It also can be rewritten as the following form based on Zuo et al. (2009),

$$\log[N(\geq \rho)] = -D\log(\rho)$$
 Eq. (3)

where  $N(\ge \rho)$  points to the number of landslides with a depth more significant than the  $\rho$  value which is the depth of landslides and D is the fractal dimension. The target data has not undergone pre-treatment and evaluation in the fractal model [42, 18, 41].

After sorting the measured depths in all landslides based on decreasing values and calculating the cumulative numbers for them, finally, the Dp-N log-log plot was generated for depth.

4. Dependence between the variables was established by the Pearson correlation coefficient (R) at the 0.05 level (Equation 4).

$$R = \frac{\sum_{i=1}^{n} (X_{i} - \overline{X})(Y_{i} - \overline{Y})}{\sqrt{\sum_{i=1}^{n} (X_{i} - \overline{X})^{2}} \sqrt{\sum_{i=1}^{n} (Y_{i} - \overline{Y})^{2}}}$$
 Eq. (4)

Where  $X_{\nu}$ ,  $Y_{\nu}$ ,  $\overline{X}$   $\overline{Y}$  and n are each observed data, estimated data equivalent to that of observed one, mean of total observed data, mean of total estimated data, and the number of data, respectively.

In that case, the coefficient of determination, R<sup>2</sup>, for each population has been calculated to show whether or not the fractal classification has been done correctly. The values

in different categories were also compared using paired and ANOVA tests.

5. To validate the results obtained by the fractal modeling, also, a total of 6 parameters which are the influential factors on landslide occurrence in the area, were considered as the input parameters consisting of the Digital Elevation Model (DEM), annual maximum daily rainfall, land-use (e.g., road, village), lithology, fault, drainage network which have been prepared by Arc-GIS 9.3.1; these parameters are influential factors on landslide occurrence in Mazandaran province [46, 47]. The quantitative parameters have been classified in the GIS environment.

### **Findings**

Statistical depth parameters of the landslides in the area have been shown in Table 1.

**Table 1)** Statistical parameters of landslide size in the area.

Statistical parameter	Depth (m)
Number	142
Mean	5.53
Std. Error of Mean	0.44
Std. Deviation	5.26
Skewness	2.74
Std. Error of Skewness	0.2
Kurtosis	9.5
Std. Error of Kurtosis	0.4
Minimum	0.6
Maximum	35
Sum	785.1

Figure 4 and Figure 5 show the Dp-N loglog plot generated for depth. Breakpoints between straight-line segments in the plot illustrate threshold values for separating various populations of depth values representing landslide differences due to different geomorphological processes. Based on the fractal modeling, five populations for depth have been obtained, as depicted in Figure 5.

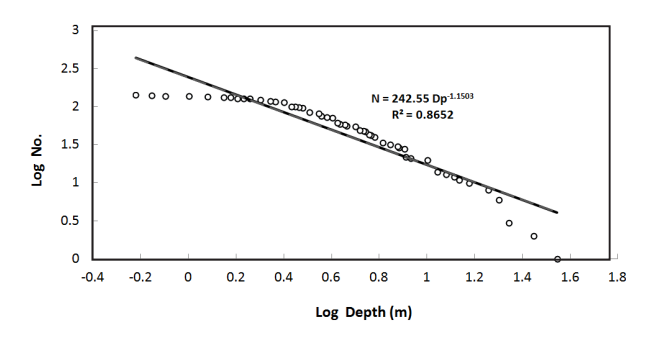


**Figure 4)** Log-log plot of Dp-N fractal model of the total landslides vs. depth.

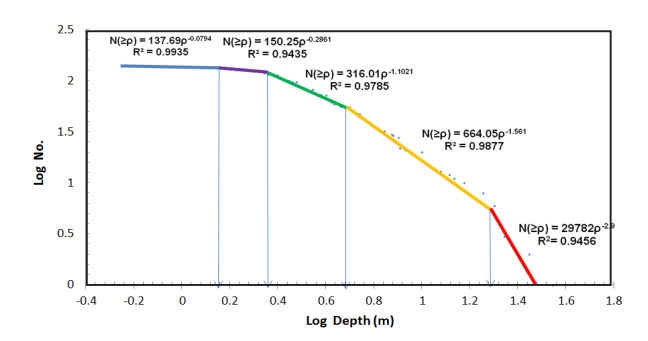


**Figure 5)** Log-log plot of Dp-N fractal model of the clustered populations of the landslides vs. depth.

A comparison of the presented models in Fig-

ure 5 with the relation between total landslides' depth and frequency before separation (Figure 4) illustrates that amount of R<sup>2</sup> significantly increased in each population of landslides.

Table 2 describes the magnitude for each separated landslide population in the study area based on the Dp-N fractal model. The table presents the difference between the separated landslide populations and the importance of considering the magnitude of landslides that could be useful for susceptibility zonation. The extreme magnitude landslides are the main ones and have depth values higher than 19.95 m, and strong landslides are determined with depth values between 5 and 19.95 m.

Amounts of P-value obtained from paired samples t-test and ANOVA test (Table 3) showed that the separate categories are significantly different at 1% (sig=0.000).

The landslides could be considered huge, and very dangerous landslides occurred in the NE, western, and SE parts of the area, as shown in Figure 6a. The strong magnitude landslides happened in most studied areas, especially NE, central, northern, NW, and western (Figure 6b). The high-magnitude landslides have depths between 2.4

**Table 2)** The magnitude for each separated landslide population in the study area based on the Dp-N fractal model.

Magnitude (m)	>19.95	5-19.95	2.4-5	1.5-2.4	0-1.5
Description	Extremely	Strongly	Highly	Moderately	Weakly
Number	6	43	65	15	13
Mean (m)	24.16	8.56	3.46	1.99	1.07
Total (m)	145	368.2	225.1	29.9	13.9

**Table 3)** Amounts of P-value obtained from paired samples t-test and ANOVA between the categories.

comparing the paired categories	Weakly Moderately	Moderately Highly	Highly Strongly	Strongly Extremely	comparing the means of different categories (ANOVA)	
Variance (F)	0.481	0.016*	0.000**	0.069	0.000**	
Mean (t-test)	0.000**	0.000**	0.000**	0.000**		

and 5 m, which occurred in the northern, NE, and NW parts of the area, as illustrated in Figure 6c.

Figures 6-a to 6-c illustrate the distribution of the extremely strong and high landslides known as anomaly ones, indicating dangerous locations due to landslide occurrences. The strong and highly magnitude landslides happened in especially NE, central, northern, NW, and western parts. Moreover, the high density of these landslides in the northern, NE, NW, and western parts of the area could be interpreted that there is a high spatial probability for happening of deep landslides.

Figure 6-f shows various landslide magnitudes distribution maps in the area. The moderately and weakly magnitude landslides could be defined as background ones that conclude low-depth ranges (Figures 6d and 6e).

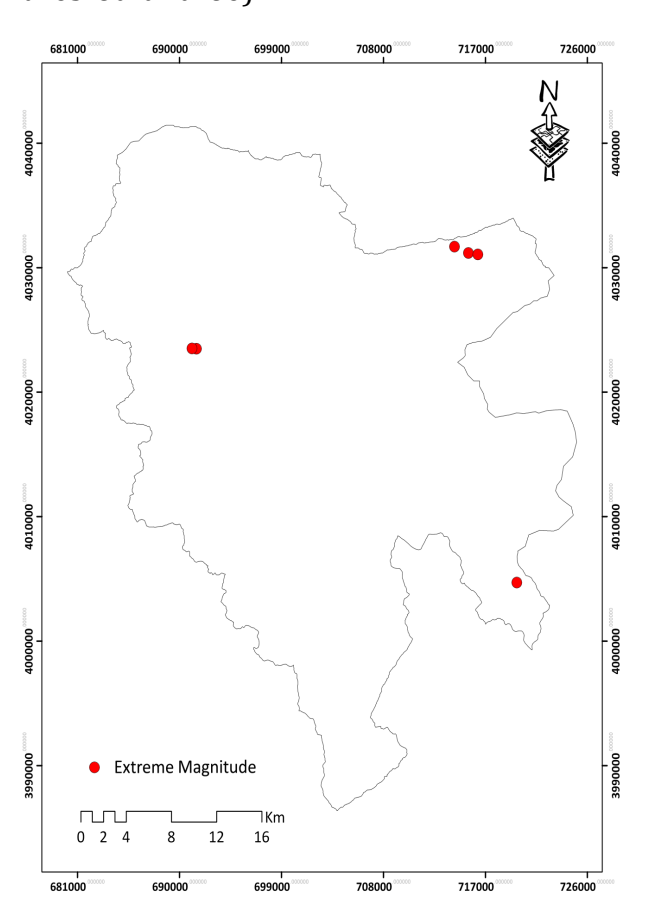


**Figure 6)** Spatial distribution of extreme landslide magnitude.

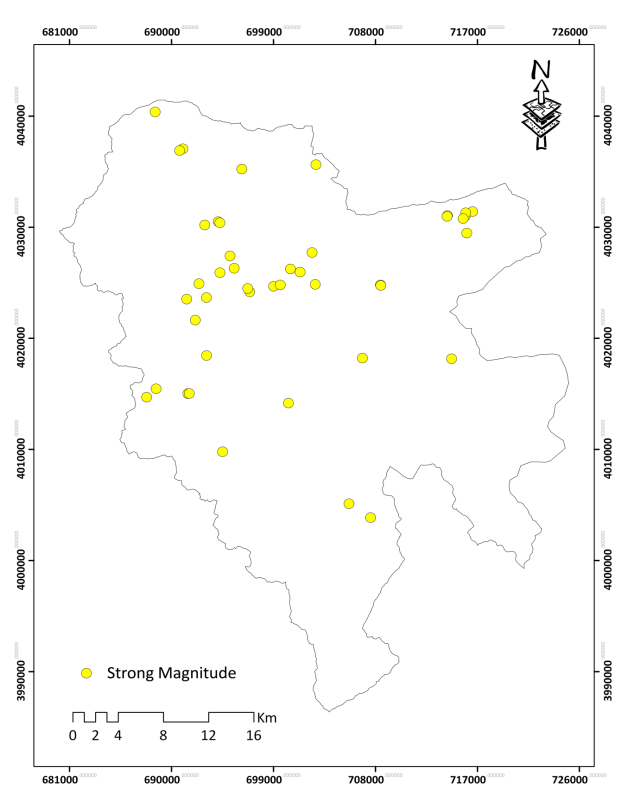


**Figure 6 Continued**) Spatial distribution of strong landslide magnitude.

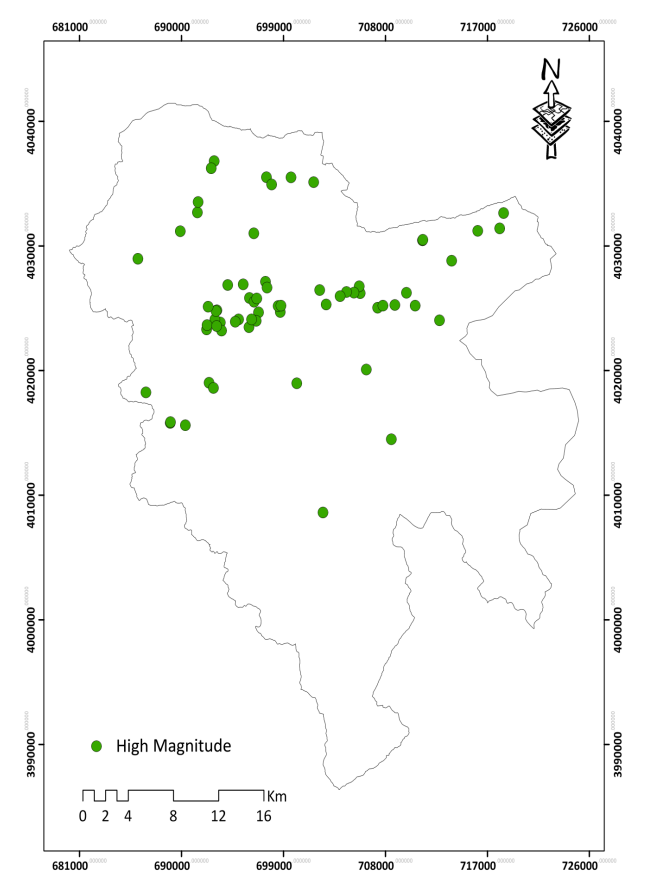


**Figure 6 Continued**) Spatial distribution of high landslide magnitude.

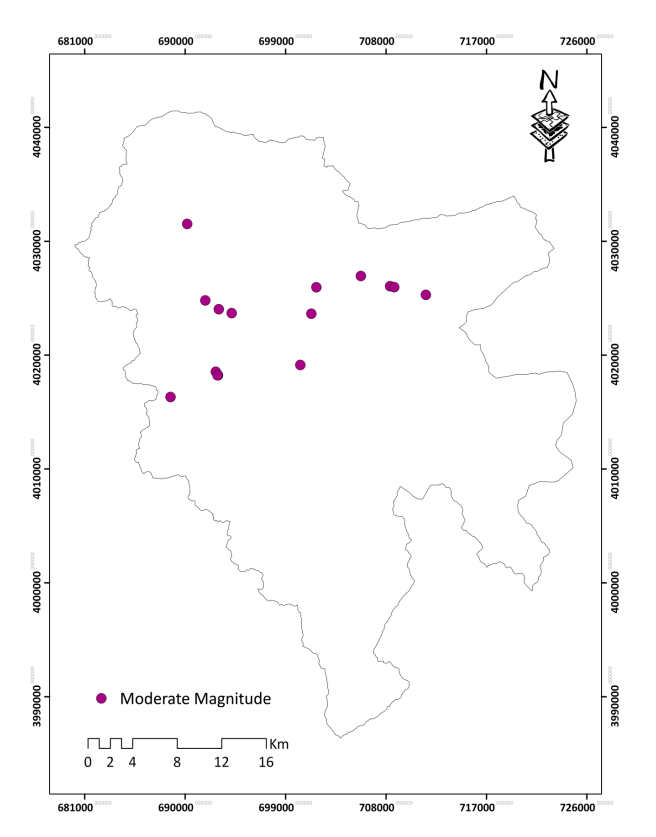


**Figure 6 Continued**) Spatial distribution of moderate landslide magnitude.

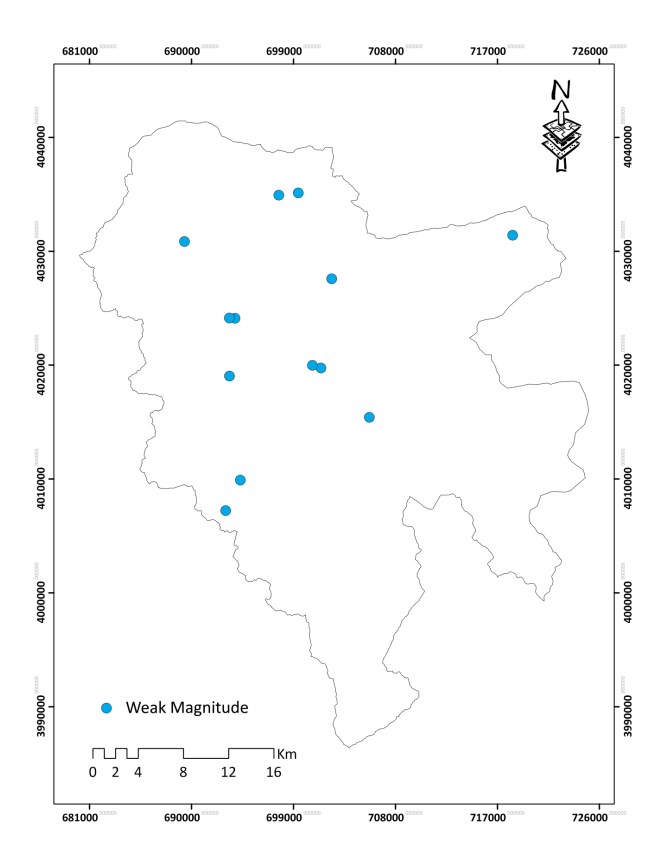


**Figure 6 Continued**) Spatial distribution of weak landslide magnitude.

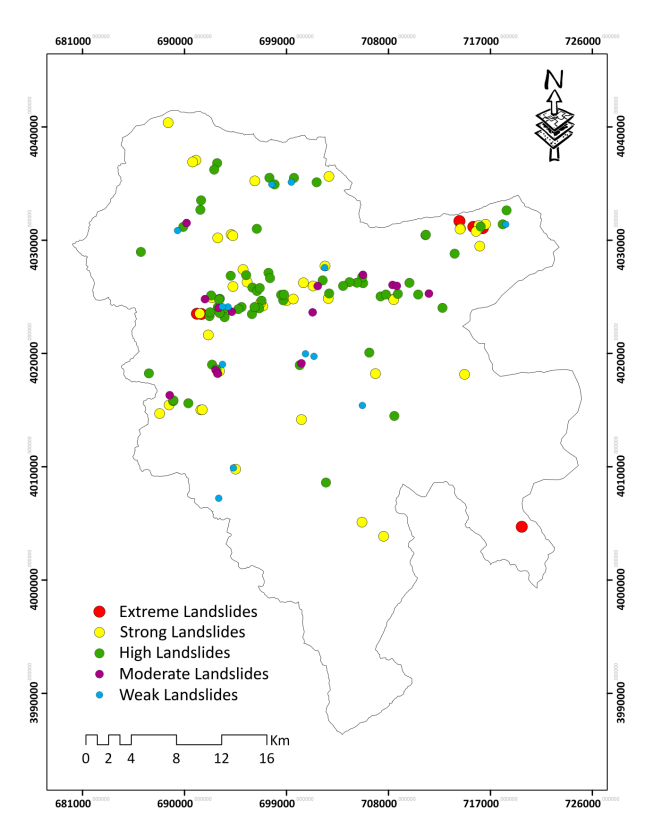


**Figure 6 Continued**) Spatial distribution of all landslide magnitude.

Correlation between the fractal model-derived results and DEM shows that the extreme magnitude landslides are located in the high elevations, especially in the NE part, which is associated with changes in land-use by human activity (Figures 7a and 7b).

All dangerous landslides correlated with agricultural lands, deforestation, gardens, roads, and villages in the studied area (Figure 7b). Furthermore, there are high ranges of annual maximum daily rainfalls (Figure 7c) and high densities of drainage networks (Figure 7d). Also, there are associated with geology (lithology and faults), as depicted in Figures 7e, 7f, and 7g.

The correlation is good in the NE, Central, and NW parts of the area, indicating a high potential for dangerous landslides.

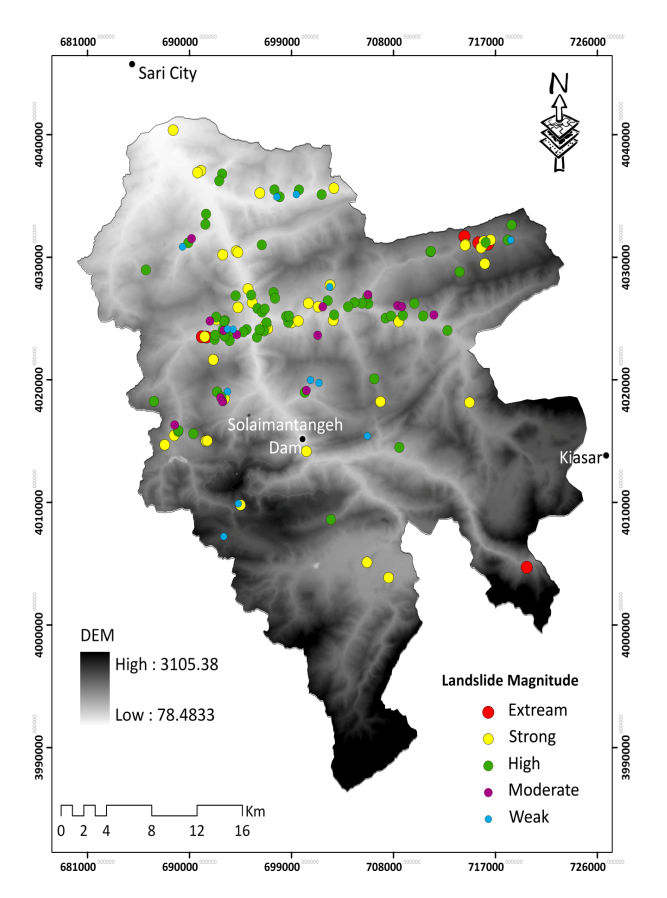


Figure 7) DEM vs. LS Magnitude.

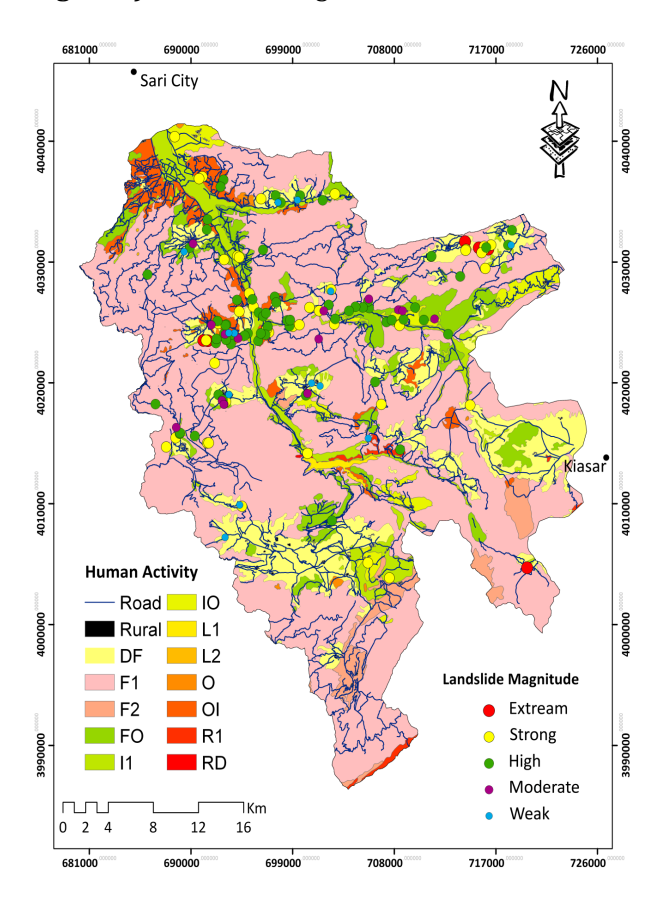
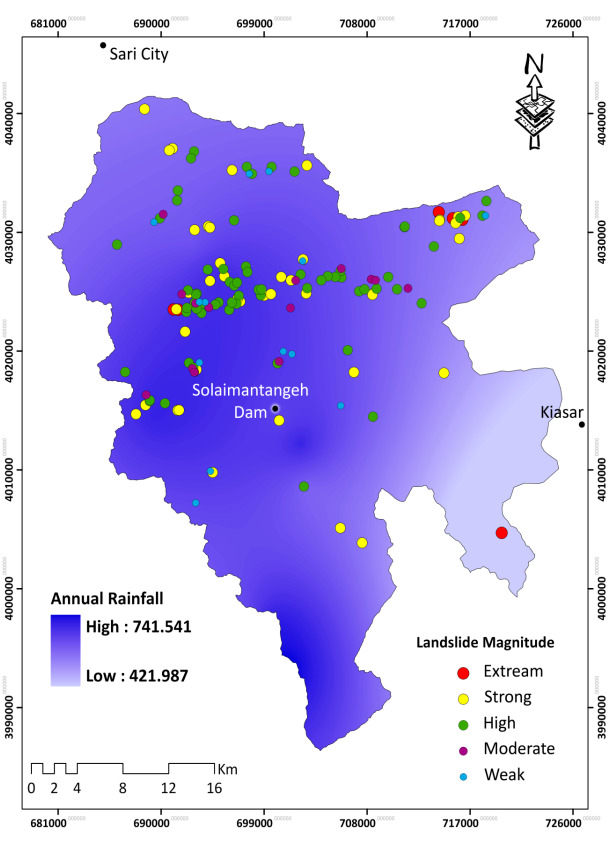


Figure 7 Continued) Human activity vs. LS Magnitude.



**Figure 7 Continued**) Annual Maximum Daily Rainfall vs. LS Magnitude.

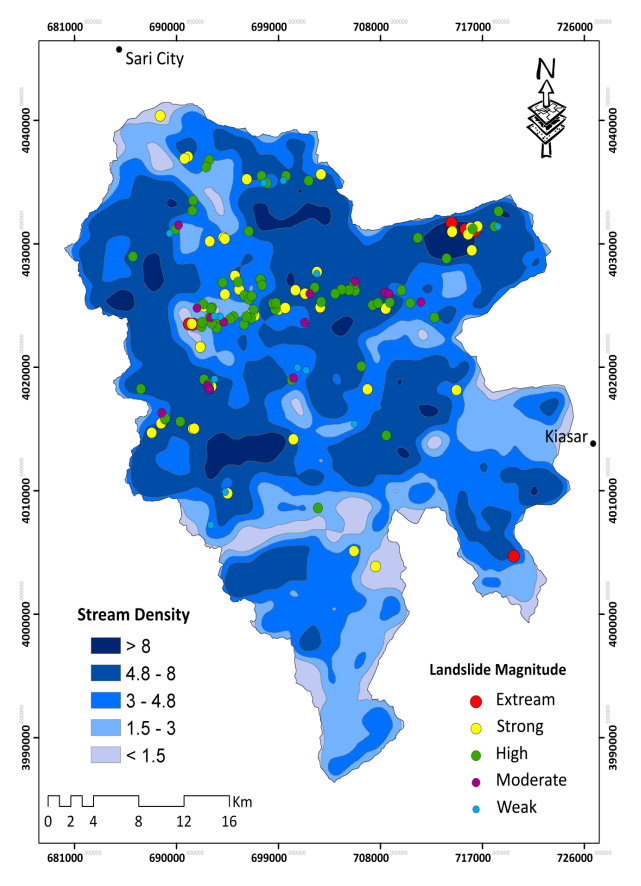


Figure 7 Continued) Stream Density vs. LS Magnitude.

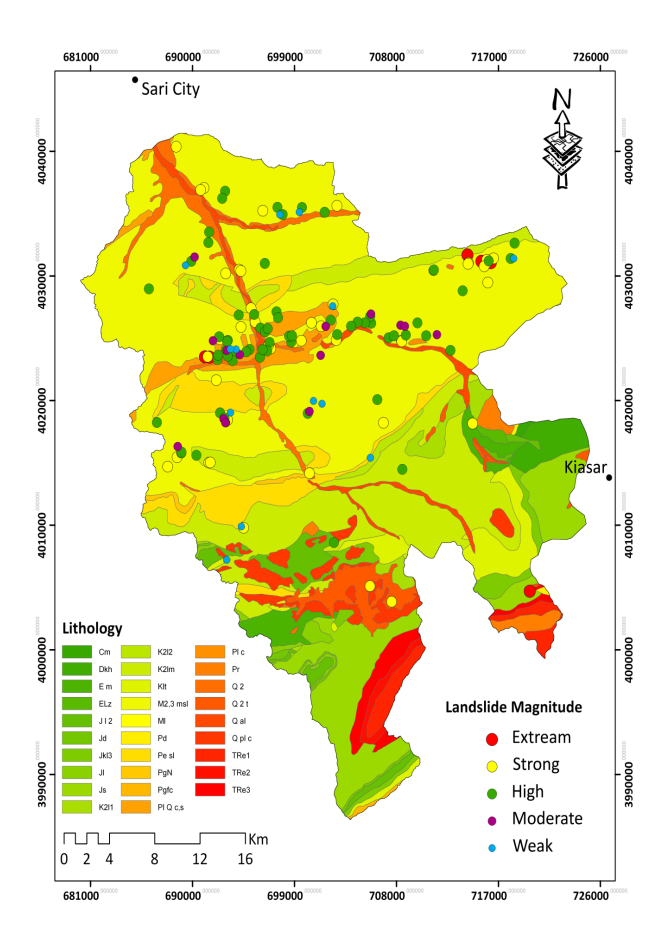


Figure 7 Continued) Lithology vs. LS Magnitude.

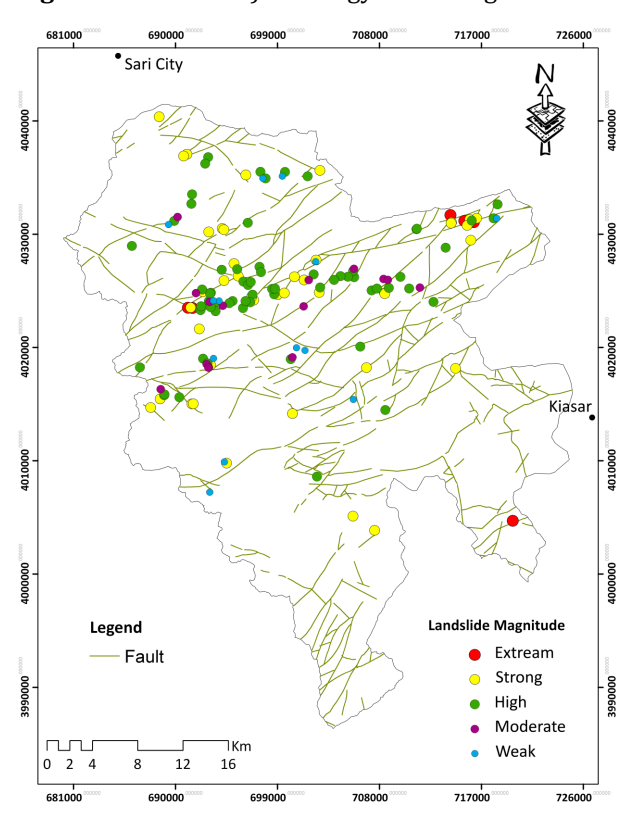
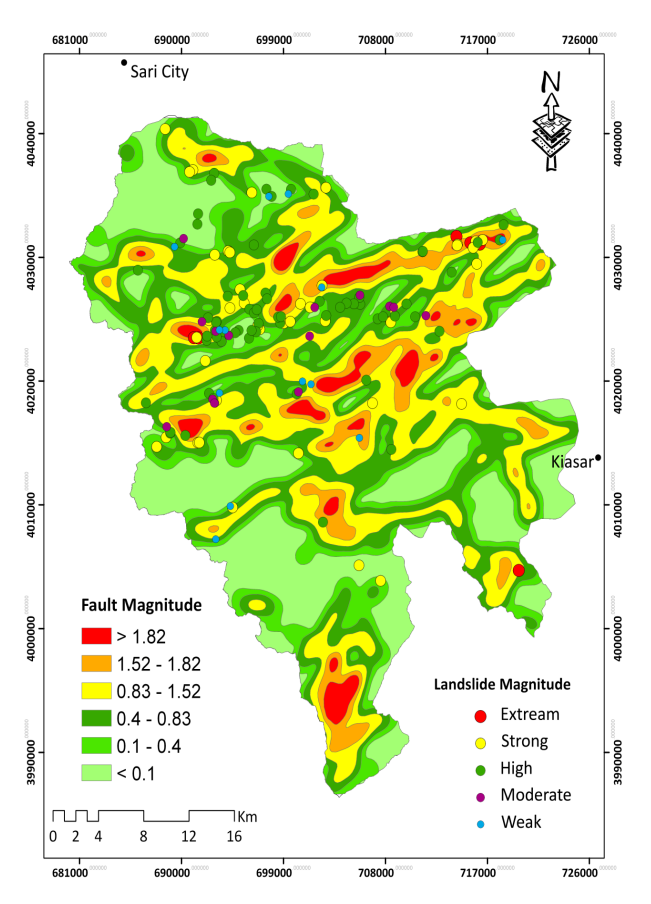


Figure 7 Continued) Faults vs. LS Magnitude.



**Figure 7 Continued**) Fault Magnitude Density vs. LS Magnitude.

### Discussion

Interpretation of Dp–N log–log plot for depth shows five landslide populations. In addition, extremely magnitude landslides were situated in the NE, central, and western areas with depth values higher than 19.95 m. The strong and highly magnitude landslides happened in the area's northern, NE, NW, and central parts, which are associated with severe landslides.

Furthermore, the annual maximum daily rainfall, land-use (including roads, villages, deforestation, garden, and agricultural lands), areas with high faults magnitude, and drainage networks density proved that accurate results could be obtained using the Dp–N fractal model; so that, extreme populations are characterized with them.

Correlation between the particulars and results obtained by the fractal modeling indi-

cates that dangerous landslides occurred in the NE, NW, and central and western parts of the area.

Separating the populations of landslides based on a parameter as magnitude, e.g., depth, must have been considered in landslide susceptibility assessment since it could have an efficient role on the weight of influential factors. On the other hand, different from mass movement classification systems (e.g., Varnez, 1978 [48]), there are different groups in a mass movement type, like slides in this research, related to the depth which can affect susceptibility, hazard, and risk investigation results, so it should be considered in landslide zonation to achieve more certainty. Fractal mathematics can define different clusters depending on landslide geometry; it is not a static classification but a kind of dynamics classification that depends on each area's physiographic and climatic situations.

### Conclusion

The study conducted on the Tajan River Basin, northern Iran, presents the potential use of the Dp–N fractal model for landslide classification as a practical tool for geomorphological studies. The improvements of this modeling rely basically on its simplicity and easy computational execution.

Correlation between the particulars and the obtained results indicates that dangerous landslides occurred in the NE, NW, central and western parts.

A fractal relationship between landslide depth (m) and the number was achieved from 142 landslide data sets and fitted to the observed data in Tajan Watershed, northern Iran. A relationship is an equation form of  $N(\geq \rho) = \rho^{-D}$  and in a similar form with low power relationships between the area and volume of landslides published by [49, 57, 46]. Guzzetti et al. (2009) mentioned that landslides suggest a self-similar behavior in dif-

ferent physiographic and climatic environments by various triggers; it refers to the fractal performance of the natural phenomena [43].

Adopting the fractal depth-number relationship of landslides would be helpful in landslide zonation [46].

### Acknowledgments

The authors acknowledge Prof. Dr. Thomas Glade from the University of Vienna (Austria) for his supervision and consultations and Mazandaran Natural Resources and Watershed Management General Office-Sari Region (Iran) for authorizing some data sets.

### References

- 1. Pardeshi S.D., Autade S.E., Pardeshi S.S. Landslide hazard assessment: recent trends and techniques. Springer Plus 2, 523. 2013; .
- Kouli M., Loupasakis C., Soupios P., Rozos D., Vallianatos F. Comparing multi-criteria methods for landslide susceptibility mapping in Chania Prefecture, Crete Island, Greece. Nat. Hazard Earth Syst. Sci. 2013; 1(1):73–109.
- 3. Zhiwang W. GIS-based methods for fractal analysis and hazard estimation of regional landslides (Ph.D. Dissertation), China University of Geosciences. 2010; 92p.
- 4. Hansen A. Landslide hazard analysis. In: Brunsden D, Prior DB, eds., Slope instability. John Wiley and Sons, New York. 1984; 523–602.
- Hansen A., Franks C.A.M. Characterization and mapping of earthquake triggered landslides for seismic zonation. Proceedings of the 4th International Conference on Seismic Zonation, Stanford, California, August 26–29, 1991; 149–95.
- 6. Mandelbrot B.B. The fractal geometry of nature. W. H. Freeman, San Francisco. 1983.
- 7. Mandelbrot B.B. How Long Is the Coast of Britain? Statistical Self-Similarity and Fractional Dimension. Science. 1967;156(3775):636-638.
- 3. Family F., Vicsek T. Dynamics of fractal surfaces. World Scientific, Singapore. 1991.
- 9. Turcotte D.L. Fractals and chaos in geology and geophysics, Cambridge University Press, Cambridge. 1997; 398 p.
- Afzal P., Dadashzadeh Ahari H., Rashidnejad Omran N., Aliyari F. Delineation of gold mineralized zones using concentration-volume fractal model in Qolqoleh gold deposit, NW Iran. Ore Geol. Rev. 2013; 55(1):125–133.

- 11. Turcotte D.L. A fractal approach to the relationship between ore grade and tonnage. Econ. Geol. 1986;81(6):1525–1532.
- Agterberg F.P., Cheng Q., Wright D.F. Fractal modeling of mineral deposits. In: Elbrond J., Tang X. (Eds.), 24th APCOM Symposium Proceeding, Montreal, Canada, 1993; 43–53.
- 13. Cheng Q., Agterberg F.P., Ballantyne S.B. The separation of geochemical anomalies from background by fractal methods. J. Geochem Explor. 1994; 51(1):109–130.
- 14. Sim B.L., Agterberg F.P., Beaudry C. Determining the cutoff between background and relative base metal contamination levels using multifractal methods. Comput. Geosci. 1999; 25(1):1023–1041.
- 15. Li C., Ma T., Shi J. Application of a fractal method relating concentrations and distances for separation of geochemical anomalies from background. J. Geochem. Explor. 2003; 77(2-3):167–175.
- 16. Carranza E.J.M. Geochemical anomaly and mineral prospectively mapping in GIS. Handbook of Exploration and Environmental Geochemistry, vol. 11. Elsevier, Amsterdam. 2008; 351.
- 17. Wang Q.F., Deng J., Wan L., Zhao J., Gong Q.J., Yang L.Q., Zhou L., Zhang Z.J. Multifractal analysis of the element distribution in skarn-type deposits in Shizishan Orefield in Tongling area, Anhui province, China. Acta. Geol. Sin. Engl. 2008; 82(4):896–905.
- 18. Zuo R., Cheng Q., Xia Q. Application of fractal models to characterization of vertical distribution of geochemical element concentration. J. Geochem. Explor. 2009; 102:37–43.
- Afzal P., Khakzad A., Moarefvand P., Rashidnejad Omran N., Esfandiari B., Fadakar Alghalandis Y. Geochemical anomaly separation by multifractal modeling in Kahang (Gor Gor) porphyry system, Central Iran. J. Geochem. Explor. 2010; 104(1-2):34-46.
- Afzal P., Fadakar Alghalandis Y., Khakzad A., Moarefvand P., Rashidnejad Omran N. Delineation of mineralization zones in porphyry Cu deposits by fractal concentration-volume modeling. J. Geochem. Explor. 2011; 108(3):220–232.
- 21. Afzal P., Fadakar Alghalandis A., Moarefvand P., Rashidnejad Omran N., Asadi Haroni, H. Application of power–spectrum–volume fractal method for detecting hypogene, supergene enrichment, leached and barren zones in Kahang Cu porphyry deposit, Central Iran. J. Geochem. Explor. 2012; 112(1):131–138.
- 22. Afzal P., Alhoseini S.H., Tokhmechi B., Kaveh Ahangaran D., Yasrebi A.B., Madani N., Wetherelt A. Outlining of high quality coking coal by concentration–volume fractal model and turning bands simulation in East-Parvadeh coal deposit, Central

- Iran. Int. J. Coal Geol. 2014; 12791):88-99.
- 23. Malamud B.D., Turcotte D.L. The applicability of power-law frequency statistics to floods. J. Hydrol. 2006; 322(1–4):168–180.
- 24. Kubota T. A study of fractal dimension of landslides. Journal of Japan Landslide Society. 1994; 31(3): 9-15.
- 25. Omura H., Hicks L.D. Fractal dimension analysis on shallow landslide and channel net system in small watershed, In Ochiai, R., ed. Proceeding of the international symposium on forest hydrology. Tokyo (IUFRO). 1994; 407-414.
- 26. Omura H. Fractal dimension analysis on spatial distribution of shallow landslides triggered by heavy rainfall. In: Proceeding of the XX IUFRO World Congress, Technical Session on Natural Disasters in Mountainous Areas. 1995; 97–104 pp.
- 27. Tarutani N., Majtan S., Morita K., Omura H. Spatial distribution pattern of rapid shallow landslides in Amakus Island. Internationales Symposion, Villach/Osterreich, Tagunqs publikation, Band 1, Seite. 2002; 317–323.
- 28. Majta'n S., Omura H., Morita K. Fractal dimension as an indicator of probability for landslides in north Matsuura, Japan. Geografický časopis. 2002; 54(1):5–19.
- 29. Yang Z.Y., Lee Y.H. The fractal characteristics of landslides induced by earthquakes and rainfall in central Taiwan. In: 10th IAEG International Congress, Nottingham. 2006; paper No. 48.
- 30. Kubota T., Omura H., Shrestha H.R. The fractal dimension of landslide group and its application to the mitigation of landslide disasters with mapping of legal restriction areas. Geophysical Research Abstracts. 2005; 7, 02170, SRef-ID: 1607-7962/gra/EGU05-A-02170.
- 31. Carranza E.J.M. Controls on mineral deposit occurrence inferred from analysis of their spatial pattern and spatial association with geological features. Ore Geol. Rev. 2009; 35(3-4):383-400.
- 32. Li Ch., Ma T., Sun L., Li W., Zheng A. Application and verification of a fractal approach to land-slide susceptibility mapping. Nat. Hazards. 2012; 61(1):169-185..
- 33. Daneshvar Saein L., Rasa I., Rashidnejad Omran N., Moarefvand P., Afzal P. Application of concentration–volume fractal method in induced polarization and resistivity data interpretation for Cu–Mo porphyry deposits exploration, case study: Nowchun Cu–Mo deposit, SE Iran. Nonlinear Proc. Geoph. 2012; 19(1):431–438.
- 34. Daneshvar Saein L., Rasa I., Rashidnejad Omran N., Moarefvand P., Afzal P., Sadeghi B. Application of Number-Size (N-S) fractal model to quantify of the vertical distributions of Cu and Mo in Nowchun porphyry deposit (Kerman, SE Iran). Arch. Min. Sci. 2013; 58 (1): 89–105.

35. Carranza E.J.M., Sadeghi M. Predictive mapping of prospectivity and quantitative estimation of undiscovered VMS deposits in Skellefte district (Sweden). Ore Geol. Rev. 2010; 38(3):219–241.

- 36. Cheng Q. Spatial and scaling modelling for geochemical anomaly separation. J Geochem. Explor. 1999; 65(3):175–194.
- 37. Goncalves M.A. Characterization of geochemical distributions using multifractal models. Math. Geol. 2001; 33(1):41–61.
- 38. Yasrebi A.B., Wetherelt A., Foster P., Coggan J., Afzal P., Agterberg F., Kaveh Ahangaran D. Application of a density-volume fractal model for rock characterisation of the Kahang porphyry deposit. Int. J Rock Mech. Min. 2014; 66(1):188–193.
- 39. Takayasu H. Fractals in the physical sciences. Manchester University Press. 1990; 176.
- 40. Ortega O.J., Marrett R., Laubach S.E. A scale-in-dependent approach to fracture intensity and average spacing measurement. AAPG Bull. 2006; 90(2):193—208.
- 41. Hassanpour Sh., Afzal P. Application of concentration–number (C–N) multifractal modeling for geochemical anomaly separation in Haftcheshmeh porphyry system, NW Iran. Arab J. Geosci. 2013; 6:957–970.
- 42. Monecke T., Monecke J., Herzi P.M., Gemmell J.B., Monch W. Truncated fractal frequency distribution of element abundance data: A dynamic model for the metasomatic enrichment of base and precious metals. Earth Planet Sc Lett. 2005; 232:363-378.
- 43. Hadian Amri M., Solaimani K., Kavian A., Afzal P., Glade T. Curve estimation modeling between area and volume of landslides in Tajan River Basin, north of Iran. ECOPERSIA 2014. 2(3):651-665.
- 44. Geology Survey of Iran (GSI). 1997; .
- 45. Guzzetti F., Ardizzone F., Cardinali M., Rossi M., Valigi D. Landslide volumes and landslide mobilization rates in Umbria, central Italy. Earth Planet. Sci. Lett. 2009; 279(3): 222–229.
- 46. Hadian Amri M. Landslides Susceptibility Modeling in a part of Tajan River Basin Using Fractal Geometry and GIS Based Methods (Doctoral dissertation). University of Mazandaran (UMZ),

- Babolsar, Iran. 2014; (In Persian).
- 47. Kelarestaghi A., Ahmadi H. Landslide susceptibility analysis with a bivariate approach and GIS in Northern Iran. Arab. J. Geosci. 2009; 2(1):95-101.
- 48. Varnes D.J. Slope movement types and processes. In: Schuster R.L. and Krizek R.J. eds., Landslides-analysis and control. National Academy of Sciences, Transportation Research Board, Special Report. 1978; 176, 11–33.
- 49. Simonett DS Landslide distribution and earth-quakes in the Bewani and Torricelli Mountains, New Guinea. In: Jennings, J.N., Mabbutt, J.A. (Eds.), Landform Studies from Australia and New Guinea. Cambridge University Press, Cambridge. 1967; 64-84.
- 50. Rice R.M., Corbett E.S., Bailey R.G. Soil slips related to vegetation, topography, and soil in Southern California. Water Resour. Res. 1969; 5(3): 647-659.
- 51. Innes J.N. Lichenometric dating of debris-flow deposits in the Scottish Highlands. Earth Surf. Proc. Land. 1983; 8(6): 579-588.
- 52. Guthrie R.H., Evans S.G. Analysis of landslide frequencies and characteristics in a natural system, coastal British Columbia. Earth Surf. Proc. Land. 2004; 29(11): 1321-1339.
- 53. Korup O. Distribution of landslides in southwest New Zealand. Landslides. 2005; 2(1): 43-51.
- 54. ten Brink U.S., Geist E.L., Andrews B.D. Size distribution of submarine landslides and its implication to tsunami hazard in Puerto Rico. Geophys. Res. Lett. 2006; 33(11): L11307.
- 55. Imaizumi F., Sidle R.C. Linkage of sediment supply and transport processes in Miyagawa Dam catchment, Japan. J. Geophys. Res. 2007;112(F3): (F03012).
- 56. Guzzetti F., Ardizzone F., Cardinali M., Galli M., Reichenbach P., Rossi M. Distribution of landslides in the Upper Tiber River basin, central Italy. Geomorphology.2008;96(1-2):105-122.
- 57. Imaizumi F., Sidle R.C., Kamei R. Effects of forest harvesting on the occurrence of landslides and debris flows in steep terrain of central Japan. Earth Surf. Proc. Land. 2008; 33(6): 827-840.